Journal of Medicinal Chemistry

Article

Synthesis and Characterization of Platinum(IV) Anticancer Drugs with Functionalized Aromatic Carboxylate Ligands: Influence of the Ligands on Drug Efficacies and Uptake

Wee Han Ang, Sbastien Pilet, Rosario Scopelliti, Franois Bussy, Lucienne Juillerat-Jeanneret, and Paul J. Dyson

J. Med. Chem., **2005**, 48 (25), 8060-8069• DOI: 10.1021/jm0506468 • Publication Date (Web): 01 November 2005

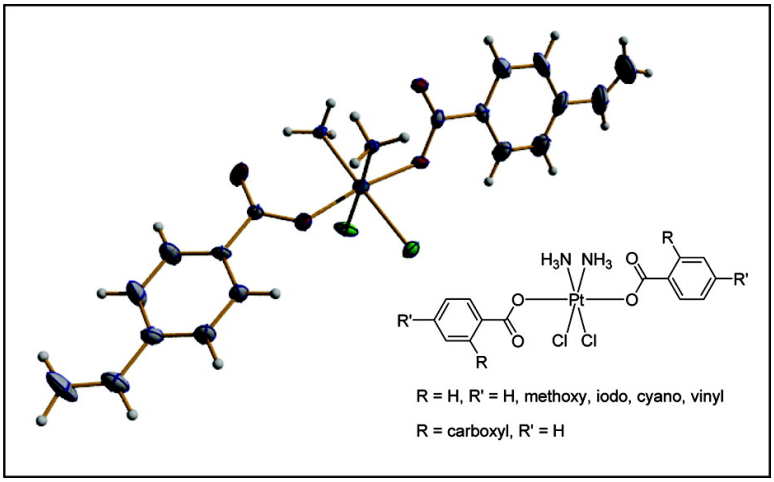

More About This Article

Additional resources and features associated with this article are available within the HTML version:

- Supporting Information
- Links to the 5 articles that cite this article, as of the time of this article download
- Access to high resolution figures
- Links to articles and content related to this article
- Copyright permission to reproduce figures and/or text from this article

View the Full Text HTML

Journal of Medicinal Chemistry is published by the American Chemical Society. 1155 Sixteenth Street N.W., Washington, DC 20036

Synthesis and Characterization of Platinum(IV) Anticancer Drugs with Functionalized Aromatic Carboxylate Ligands: Influence of the Ligands on Drug Efficacies and Uptake

Wee Han Ang,[†] Sébastien Pilet,[‡] Rosario Scopelliti,[†] François Bussy,[‡] Lucienne Juillerat-Jeanneret,*[,§] and Paul J. Dyson*[,†]

Institut des Sciences et Ingénierie Chimiques, Ecole Polytechnique Fédérale de Lausanne (EPFL), CH 1015 Lausanne, Switzerland, Institut de Minéralogie et Géochimie, Université de Lausanne (UNIL), CH 1015 Lausanne, Switzerland, and University Institute of Pathology, Centre Hospitalier Universitaire Vaudois (CHUV), CH 1011 Lausanne, Switzerland

Received July 7, 2005

A series of *trans*-platinum(IV) complexes with functionalized aromatic carboxylate ligands, *cis*,*cis*,*trans*-$Pt(NH_3)_2Cl_2(CO_2C_6H_4R)_2$ (R = H **(3)**, *p*-vinyl (**4**), *p*-methoxy (**5**), *p*-iodo (**6**), *p*-cyano (**7**), or *o*-carboxyl (**8**)) was synthesized and characterized by spectroscopic methods. Crystal structures of **3**, **4**, **7**, and **8** were obtained, which revealed that their structural conformations were influenced by intramolecular H-bonding interactions. The complexes were evaluated for cellular uptake and inhibition of cell proliferation against a panel of lung, colon, and breast carcinoma cell lines. The functionalization of the aromatic carboxylate ligand was found to have a profound influence on the uptake, and hence, efficacy, of this class of complex.

Introduction

Since its discovery almost four decades ago, cisplatin (Figure 1) has become one of the most widely used anticancer drugs with a broad activity range against many tumors.[1−3] The generally accepted mode of action of cisplatin arises from its binding to DNA,[3−5] and the failure of repair mechanisms to remove Pt−DNA adducts subsequently triggers apoptotic cellular suicide.[3,4] Consequently, interest in this field led to the development of cisplatin analogues, such as carboplatin, oxaliplatin, and nedaplatin, further improving the efficacy of platinum-based chemotherapy and extending the scope of its clinical application.[2,3,6] However, the incidence of drug resistance, acquired or intrinsic, continues to limit the effectiveness of platinum-based chemotherapy. Cisplatin-associated drug resistance is attributable to a number of factors, such as reduced cellular drug uptake or increased drug efflux, enhanced repair mechanism, drug deactivation, or a combination of the above-mentioned mechanisms.[3,4]

One strategy used to overcome resistance is to design and build specific functionalities onto platinum compounds to enhance uptake via drug targeting or to inhibit resistance mechanisms. Platinum(II) complexes have been used,[7] although structural limitations, principally their lower coordination number and the need to maintain the *cis*-diamine geometry around the platinum center to maximize cytotoxicity,[8] severely limits their usefulness. In that respect, Pt(IV) complexes, with their two additional coordination sites, offer greater synthetic flexibility. In particular, Lippard et al. have demonstrated that a Pt(IV)−estrogen complex, formed by conjugating an estrogen derivative via a succinate linker onto a *trans*-Pt(IV) carboxylate structure, was able to sensitize estrogen-receptor(+) mammalian tumor cells to treatment (Figure 1).[9] We have subsequently shown that a Pt(IV)−ethacrynic acid complex could inhibit the activity of glutathione-S-transferase, a multidrug resistance enzyme, in vitro.[10] Lippard also proposed the *trans*-Pt(IV) carboxylate as a design framework for the incorporation of functional groups into platinum-based compounds.[9] From a design perspective, this is an attractive synthetic strategy, because *trans*-Pt(IV) carboxylates were found to be rapidly reduced under physiological conditions by biological reducing agents, such as glutathione, to release the functionalized ligands and yield cytotoxic Pt(II) species.[11] Significantly, the prototype Pt(IV) complex, satraplatin (Figure 1), entered Phase III clinical trials in 2001 as an orally active anticancer drug for the treatment of hormone-

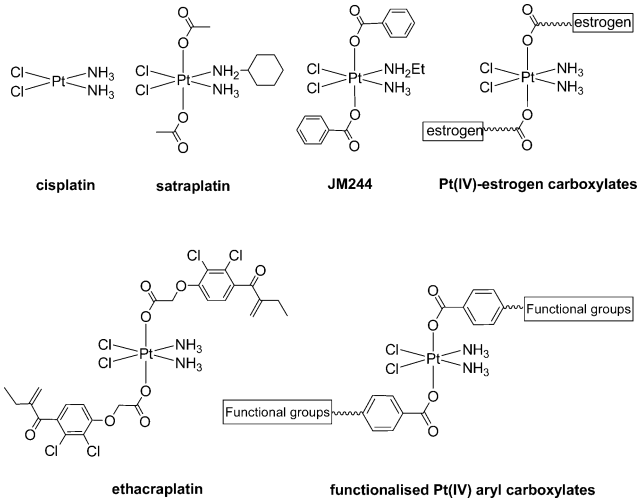

Figure 1. Structures of cisplatin−platinum(IV) complexes with proven anticancer activity and proposed functionalized Pt(IV) carboxylates.

* Corresponding authors: Dr. Lucienne Juillerat-Jeanneret, phone: +41 21 314 7173, fax: +41 21 314 7115, e-mail: lucienne.juillerat@chuv.ch; Prof. Paul J. Dyson, phone: +41 21 693 9854, fax: +41 21 693 9885, e-mail: paul.dyson@epfl.ch.
[†] Institut des Sciences et Ingénierie Chimiques.
[‡] Université de Lausanne.
[§] University Institute of Pathology.

10.1021/jm0506468 CCC: $30.25
Published on Web 11/01/2005

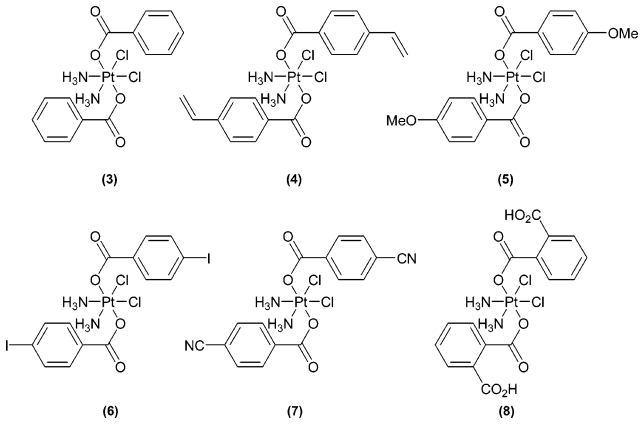

Figure 2. Structures of target complexes **3**−**8**.

refractory prostate cancer, and it remains under intensive clinical evaluation.[12]

Aryl groups have been shown to improve the uptake of drugs by conferring greater lipophilicity and facilitating transport across cell membranes. For example, it was found that aryl ethers of functionalized glycomers are effective growth inhibitors and induce apoptosis in human glioblastoma cells.[13] Similarly, benzoyl derivatives of pyrrolidine-3,4-diol were found to improve the growth-inhibitory properties of the parent compounds against human glioblastoma and melanoma cells.[14] In addition, aromatic rings provide a scaffold on which desirable functional groups can be easily built and manipulated. As part of our ongoing work to build functionalized Pt(IV) carboxylate complexes, we have studied the effect of functional group modification on the drug efficacy of *trans*-Pt(IV) aryl carboxylate compounds. We have also obtained crystal structures of some of the complexes studied that, to the best of our knowledge, are the first reported structures of this important class of anticancer compound. The cellular uptake and growth-inhibitory properties of these complexes were evaluated in human tumor cells.

Results and Discussion

Only a few *trans*-Pt(IV) aryl carboxylates have been reported,[15−17] with JM244 (Figure 1) having been studied extensively.[17,18] The spectroscopic characteristics of this class of complexes have not been analyzed in detail, and no solid-state structures have been reported. Harrap et al. have screened several JM244-type complexes, with varying amine ligands, against a panel of leukemia and ovarian cell lines and found them to be more cytotoxic than their alkoyl counterparts, accumulating more strongly in cisplatin-sensitive and -resistant cell lines.[17,18] Besides conferring lipophilicity, the effect of the benzoyl ligand on the efficacy of the Pt(IV) complex is not well understood. To better understand these effects, as part of our ongoing study on functionalized Pt(IV) carboxylates, we have synthesized and studied a series of *trans*-Pt(IV) aryl carboxylate complexes with various functional groups attached to the aryl moiety (Figure 2). Benzoyl ligands with different para substituents were selected, including vinyl-, methoxy-, iodo-, and cyano-, and compared to the prototype $[Pt(NH_3)_2Cl_2(CO_2Ph)_2]$. In the course of this study, a facile method of synthesizing the *trans*-Pt(IV) 2-carboxyl-benzoate derivative was found.

Scheme 1. Synthetic Route Used to Prepare Pt(IV) Aryl Carboxylate Complexes

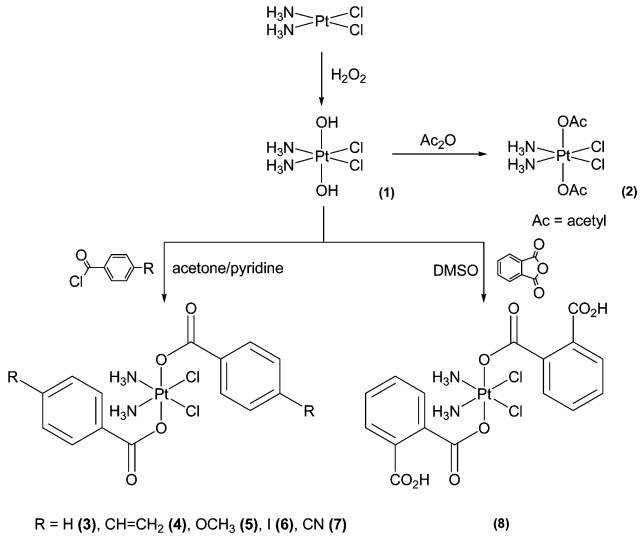

The target compounds were synthesized by acylation of dihydroxylplatinum(IV) **1** using either the acid chlorides or acid anhydrides of the targeted carboxylic acids, as shown in Scheme 1. Reactions with acid chlorides were carried out in the presence of pyridine (as a base) in a method described by Galanski et al., which had previously been successfully applied to a series of *trans*-Pt(IV) carboxylates.[16] We found that the reaction conditions could be applied to functionalized benzoic acids, although the reaction yields tend to vary according to the type of functional group. The products, viz $[Pt(NH_3)_2Cl_2(p\text{-}CO_2C_6H_4{-}H)_2]$ **3**, $[Pt(NH_3)_2Cl_2(p\text{-}CO_2C_6H_4{-}CH{=}CH_2)_2]$ **4**, $[Pt(NH_3)_2Cl_2(p\text{-}CO_2C_6H_4{-}OCH_3)_2]$ **5**, $[Pt(NH_3)_2Cl_2(p\text{-}CO_2C_6H_4{-}I)_2]$ **6**, and $[Pt(NH_3)_2Cl_2(p\text{-}CO_2C_6H_4{-}CN)_2]$ **7**, were poorly soluble in water, which was used extensively to remove the pyridinium byproducts. In addition, because precursor **1** was found to be insoluble in polar organic solvents, such as THF and DMSO, the products could be easily separated and purified by dissolution in a suitable polar solvent such as THF, followed by filtration and reprecipitation.

For the synthesis of $[Pt(NH_3)_2Cl_2(o\text{-}CO_2C_6H_4{-}CO_2H)_2]$ **8**, a range of reaction and solvent conditions were explored. The use of polar organic solvents, such as THF or acetone, did not result in the formation of **8**, and the use of molten phthalic anhydride resulted in discoloration and slight decomposition. Conducting the reaction in dry DMSO, followed by workup with water, afforded **8** in good yield. A possible explanation for this observation could be the favorable thermodynamics resulting from the formation of highly soluble Pt(IV) carboxylates from the less soluble precursor. In keeping with the *trans*-Pt aryl carboxylates, compound **8** was also found to be only slightly soluble in water.

All complexes were characterized using IR, ^1H and ^{195}Pt NMR spectroscopy, and nanospray ionization mass spectrometry (NSI-MS) (see Tables S-1 and S-2, Supporting Information). The IR spectra of all the complexes show characteristic ammine N−H stretches within the region of 3000−3200 cm^{-1}. In addition, the carboxylate C=O stretches in the Pt(IV) complexes were observed at lower frequencies (typically 50−100 cm^{-1}) compared to those of the free acid, suggesting, as expected, a

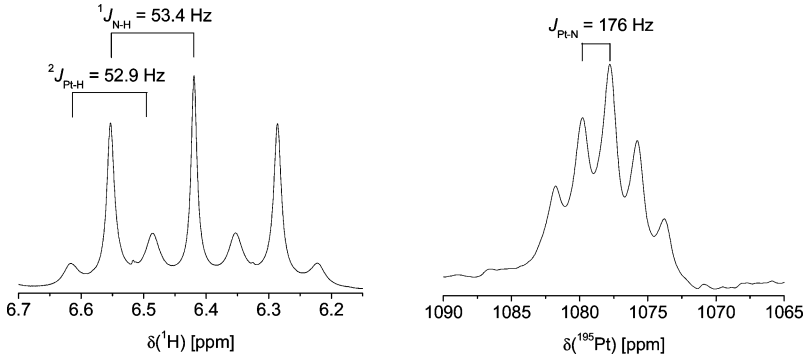

Figure 3. ^{1}H NMR (left) and ^{195}Pt−{^{1}H} NMR (right) spectra of complex **4**.

weakening in the C═O bond. A similar trend has been observed in other reported *trans*-Pt(IV) carboxylate complexes.[15,16,19,20] Negative mode NSI-MS was found to be very useful for the identification of complexes **3**−**8**.[21] Using diluted methanolic solutions, the neutral compounds often yield the parent $[M - H]^-$ peak with the highest relative intensity along with other signature mass peaks attributable to either solvated or aggregated species. Fragmentation analyses of the parent peaks resulted in the loss of NH_3, HCl, and carboxylate ligands, which is consistent with their proposed molecular structures.

The ^{1}H NMR spectra of the complexes could be assigned by comparison with the spectra of the parent acid. With the exception of **3** and **8**, the aromatic proton resonances were observed as an AA′BB′-system, consistent with the structure of para-disubstituted aromatic rings that are chemically equivalent. Likewise for complex **3** and **8**, the aromatic resonances correspond to the structures of monosubstituted and ortho-disubstituted aromatic rings, respectively. In deuterated DMSO, the ammine proton resonances are observed as a broadened peak, due to coupling to the quadrupolar ^{14}N nuclei, between 6 and 6.5 ppm. In deuterated THF, however, spin-to-spin coupling of ammine protons to quadrupolar ^{14}N nuclei ($^1J_{HN}$ = 53−54 Hz) could be observed, as well as coupling to the ^{195}Pt nucleus ($^2J_{HPt}$ = 52−56 Hz) (Figure 3). Spin-to-spin coupling between ^{14}N and ^{195}Pt nuclei was also observed in the proton-decoupled ^{195}Pt NMR spectrum ($^1J_{PtN}$ = 172−179 Hz), which revealed a 1:2:3:2:1 quintet, implying that there is coupling to two spin-1 nuclei (^{14}N). The effects of deuterium exchange were ruled out as the same spectra were observed when the experiments were conducted in undeuterated THF. It is highly unusual that coupling to the quadrapolar ^{14}N atom is so well-resolved, but this phenomenon could have been a result of slow relaxation of the ^{14}N nuclei due to the high symmetry within the spin system and rapid molecular reorientation, possibly due to the ammine ligand spinning rapidly around its Pt−N bond axis. Such rapid rotation had been observed even in solid samples of ^{15}N-enriched Pt−amine complexes as part of solid-state NMR studies.[22] The similar values in coupling constants of $^1J_{NH}$ and $^2J_{PtH}$ also resulted in an overlap of the peaks, leading to much simplified spectra for the complex coupling system.

Characterization of 3, 4, 7, and 8 in the Solid State. Single crystals of **3**, **4**, **7**, and **8** suitable for X-ray diffraction analysis were grown by vapor diffusion of pentane into the THF solutions of the complexes. Ortep views of the structures are shown in Figure 4, and selected bond distances are provided in the caption. Crystallographic data of **3**, **4**, **7**, and **8** are given in Table 1.

There have been numerous reports on the structures of various Pt(IV) alkyl carboxylates; however, to the best of our knowledge, X-ray structures of Pt(IV) aryl carboxylates are not available. Nevertheless, the bonding parameters in **3**, **4**, **7**, and **8** were found to be similar to those reported for Pt(IV) alkyl carboxylates (see Table S-3, Supporting Information).[19,23,24] The coordination sphere around the Pt center constitutes a distorted octahedron, with two N and two Cl atoms, bonded *cis*-with respect to each other to the Pt center, occupying the equatorial plane. The axial O−Pt−O bonds are slightly bent, caused by intramolecular H-bonding between the ammine protons and the carboxylate O atoms. The distances of the Pt−Cl, Pt−N, and Pt−O bonds in all the structures are similar and are not too different from those reported for Pt(IV) alkyl carboxylates.[19,20,23] Structurally, complex **8** is significantly different from **3**, **4**, or **7**. The carboxylate bond adjacent to the Pt center is oriented almost perpendicular to the aromatic ring, in contrast to the carboxylate bonds of **3**, **4**, and **7**, which are coplanar to their respective aromatic rings. Although this geometry would disrupt the conjugated system between the aromatic ring and the Pt-bonded carboxyl ligands, such a conformation allows the ortho carboxyl O atom to be H-bonded to an ammine proton. For complexes **3**, **4**, and **7**, as there are no ortho functional groups, the conformations are driven only by H-bonding interactions of the Pt-carboxyl O atom to the ammine protons. In these three structures, one carboxylate bond is H-bonded to two ammine protons with the other H-bonded to one ammine proton.

Drug Efficacy and Accumulation. The efficacy on cell-growth inhibition of the control molecule, cisplatin, and complexes **2**−**8** was screened against a panel of lung, colon, and breast carcinoma cell lines using the MTT test, which measures mitochondria dehydrogenase activity as a marker of cell viability (Table 2).[25] Complexes **3**−**6** were 5−20-fold more cytotoxic than cisplatin, whereas complexes **7** and **8**, which are structurally similar, were much less efficacious. The *trans*-diacetyl Pt(IV) complex **2** was also found to be non-cytotoxic in the cell lines tested. Drug accumulation of the complexes over a continuous 6 h exposure was further quantified using inductively coupled plasma mass spectrometry (ICP-MS) (Table 2). Drug uptake was observed to be relatively high in cells treated with

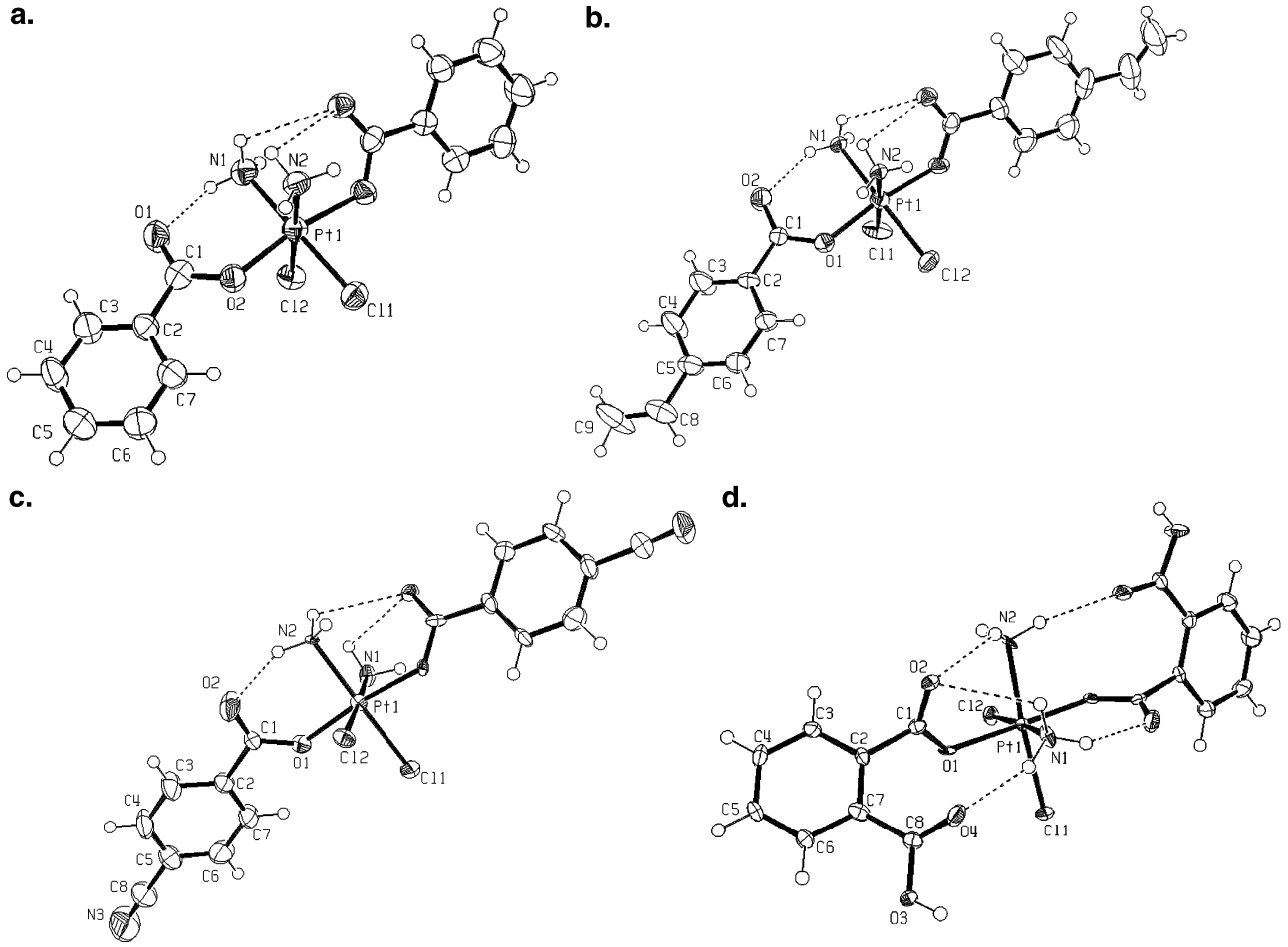

Figure 4. (a–d) Ortep representation of complexes **3**, **4**, **7**, and **8**. (a) Ortep representation of **3**; thermal ellipsoids are 50% equiprobability envelopes, with hydrogen atoms as spheres of arbitrary diameter. Key bond lengths (Å) and angles (deg): Pt–O_{avg}, 2.01(1); Pt–N_{avg}, 2.05(1); Pt–Cl_{avg}, 2.30(1); C1–$O1_{avg}$, 1.30(2); C1–$O2_{avg}$, 1.22(2); C1–$C2_{avg}$, 1.50(2); O–Pt–O, 170.9(2); N–Pt–Cl_{avg}, 179.2(4). (b) Ortep representation of **4**; thermal ellipsoids are 50% equiprobability envelopes, with hydrogen atoms as spheres of arbitrary diameter. Key bond lengths (Å) and angles (deg): Pt–O_{avg}, 2.00(1); Pt–N_{avg}, 2.05(2); Pt–Cl_{avg}, 2.31(1); C1–$O1_{avg}$, 1.29(2); C1–$O2_{avg}$, 1.22(2); C1–$C2_{avg}$, 1.50(1); O–Pt–O, 172.2(2); N–Pt–Cl_{avg}, 177.5(4). (c) Ortep representation of **7**; thermal ellipsoids are 50% equiprobability envelopes, with hydrogen atoms as spheres of arbitrary diameter. Key bond lengths (Å) and angles (deg): Pt–O_{avg}, 2.01(2); Pt–N_{avg}, 2.07(2); Pt–Cl_{avg}, 2.32(1); C1–$O1_{avg}$, 1.30(3); C1–$O2_{avg}$, 1.23(3); C1–$C2_{avg}$, 1.50(3); O–Pt–O, 173.0(3); N–Pt–Cl_{avg}, 177.8(5). (d) Ortep representation of **8**; thermal ellipsoids are 50% equiprobability envelopes, with hydrogen atoms as spheres of arbitrary diameter. Key bond lengths (Å) and angles (deg): Pt–O_{avg}, 2.00(1); Pt–N_{avg}, 2.05(2); Pt–Cl_{avg}, 2.30(1); C1–$O1_{avg}$, 1.29(2); C1–$O2_{avg}$, 1.24(2); C1–$C2_{avg}$, 1.51(3); O–Pt–O, 173.3(3); N–Pt–Cl_{avg}, 175.9(4).

complexes **3**–**7** and much lower for cisplatin, **2**, and **8**. This observation suggests a strong relationship between drug efficacy and uptake and possibly the dominant factor concerning the efficacy of this class of complex, although Pt(IV) carboxylates have been known to be affected by other factors such as reduction potential, reactivity toward thiols, etc.[26] In addition, the lipophilicity of the compounds does not fully rationalize the uptake trend. Although there is an overall correlation between complex accumulation and the lipophilicity of the benzoic ligands present in the complex (see Table 2, log P_{oct} values),[27] indicating that liphophilicity does play a role, the correlation is only moderate, alluding to the fact that there could be more complex drug–membrane interactions that cannot be adequately accounted for by the octanol–water partition model. For compound **8** in particular, the poor activity could be a consequence of the acidic carboxylic proton dissociating in the culture media, yielding a charged species that does not easily penetrate the hydrophobic cellular membrane. In the absence of an active transport mechanism, passive diffusion is only likely to result in very low levels of **8** traversing the lipid layer.

To investigate the drug uptake mechanism, time-dependent drug uptake by A549 cells was evaluated following 6, 24, 48, and 72 h exposure to complexes **3**–**7** (Figure 5). Complexes **4** and **5** demonstrated the highest Pt intracellular levels. The results, however, did not fully account for the observation of the poor efficacy of **7**. To investigate this anomaly, treated cells were extracted, and both the cytosol and the resulting cell debris, comprising mainly the cellular membrane layer, were analyzed for Pt content (Figure 6) to determine the amount of drug traversing the cellular membrane. In A549 cells, **7** accumulated mainly in the membrane fraction rather than the cytosol, which could explain its poor efficacy. A possible explanation is that cyano groups interacted strongly with the membrane lipid layer, causing the complex to be trapped in the cellular membrane, preventing its diffusion into the cytoplasm. Conversely, complex **4** accumulated much more strongly in the cytosol, presumably due to the inert hydrophobic

Table 1. Crystallographic Data for Complexes **3**, **4**, **7**, and **8**

	3	**4**	**7**	**8**
chem. formula	$C_{22}H_{32}Cl_2N_2O_6Pt$	$C_{26}H_{36}C1_2N_2O_6Pt$	$C_{24}H_{30}Cl_2N_4O_6Pt$	$C_{20}H_{24}Cl_2N_2O_9Pt$
F_w	686.49	738.56	736.51	702.40
crystal system	monoclinic	monoclinic	triclinic	triclinic
space group	$P2_1/c$	$I2/a$	$P\bar{1}$	$P\bar{1}$
a (Å)	7.7485(8)	23.951(2)	7.8196(8)	8.9038(7)
b (Å)	18.294(3)	7.8455(13)	12.2969(11)	12.4327(12)
c (Å)	18.356(4)	32.732(3)	16.4366(15)	12.8543(14)
α (°)	90	90	81.492(8)	62.590(11)
β (°)	92.129(11)	110.353(8)	77.063(8)	82.906(8)
χ (°)	90	90	88.498(7)	72.039(9)
volume (Å^3)	2600.2(7)	5766.6(12)	1523.4(2)	1201.4(2)
Z	4	8	2	2
D_{calc} (g cm^{-3})	1.754	1.701	1.606	1.942
F(000)	1352	2928	724	684
μ(mm^{-1})	5.640	5.093	4.821	6.115
temp (K)	140(2)	140(2)	140(2)	140(2)
wavelength (Å)	0.71073	0.71073	0.71073	0.71073
measured reflns	15394	15496	9051	7047
unique reflns	4426	4907	4706	3727
unique reflns [$I>2\sigma(I)$]	3364	3828	4166	3476
no. of data/restraints/parameters	4426/12/302	4907/14/395	4706/32/354	3727/0/309
R^a [$I>2\sigma(I)$]	0.0485	0.0537	0.060	0.0516
$wR_2{}^a$ (all data)	0.1003	0.1172	0.1602	0.1502
GooF^b	1.166	1.162	1.172	1.182
largest diff. peak/hole (e/Å^3)	4.150/−1.629	1.416/−1.841	3.336/−1.732	3.558/−2.928

[a] $R = \Sigma||F_o| - |F_c||/\Sigma|F_o|$, $wR_2 = \{\Sigma[w(F_o^2 - F_c^2)2]/\Sigma[w(F_o^2)^2]\}^{1/2}$. [b] GooF $= \{\Sigma[w(F_o^2 - F_c^2)2]/(n - p)\}^{1/2}$ where n is the number of data and p is the number of parameters refined.

Table 2. In Vitro Drug Efficacy and Drug Uptake for Cisplatin and Complexes **2**−**8**

	IC_{50} [μM][a]				Pt uptake [μg Pt/mg protein][b]		log P_{oct}[c]
	A549	HT29	MCF7	T47D	A549	HT29	
cisplatin	31.43	16.82	36.02	58.52	below det. limit	0.01 ± 0.00	−
2	>80	>80	>80	>80	0.35 ± 0.01	0.01 ± 0.00	−
3	1.57	2.03	2.24	1.77	2.27 ± 0.03	2.27 ± 0.02	1.87
4	1.66	2.27	0.77	1.42	5.88 ± 0.05	3.85 ± 0.03	2.61
5	1.77	2.23	1.41	1.97	3.23 ± 0.03	6.14 ± 0.05	3.02
6	3.30	4.72	1.82	2.07	3.16 ± 0.02	3.75 ± 0.03	1.96
7	15.30	83.24[d]	>80	>80	5.93 ± 0.04	3.62 ± 0.03	1.56
8	>80	>80	>80	>80	0.10 ± 0.01	0.02 ± 0.01	0.70

[a] Data values presented are based on experiments after 72 h exposure. [b] Data values presented are based on experiments conducted on A549 lung and HT29 colon carcinoma at [10 μM] over 6 h exposure. [c] Values presented are the partition coefficient of the parent benzoic acid ligand obtained from literature,[27] except for **4**, which was calculated using the Bio-Loom software v1.0 from Biobyte Corp. [d] Based on extrapolated data.

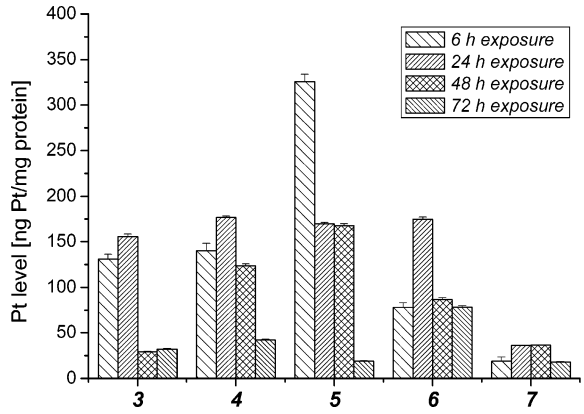

Figure 5. Uptake of **3**−**7** by A549 lung carcinoma cells. Cells were grown to confluence, then fresh medium containing drugs at 1 μM were added for 6, 24, 48, and 72 h. Pt levels of the harvested cells were quantified using ICP-MS.

vinyl group. Similar observations were made in HT29 cells.

A more detailed time course study on the drug efficacy of complexes **3**−**6** was conducted to examine the dose−response effect over different exposure times (Figure 7 and S-1). Complexes **3**−**6** were effective within 24 h of exposure and were much more rapidly efficacious in the inhibition of cell growth than cisplatin, which required up to 48 h to be effective. In addition, the IC_{50} values of complexes **3**−**6** were also much lower than that of cisplatin. These results were consistent with the findings of the time-dependent uptake studies and with previous reports.[17] The main increase in drug uptake occured within 24 h; thereafter, drug uptake stabilized and decreased. This corresponds to the observation that after 24 h, the toxicity of the complexes increased only marginally, suggesting a saturation effect during which the drug uptake and efflux reached equilibrium. In addition, the uptake profiles were bell-shaped, with a general decline in Pt levels after 24 h of exposure, confirming previous observations and suggesting that some form of efflux mechanism could have taken place.[28]

The cells were therefore screened for P-glycoprotein (Pgp) activity, a multidrug resistance (MDR) efflux membrane protein, using the calcein uptake assay with verapamil, a Pgp inhibitor.[29] A549 and HT29 cells were first treated with verapamil and then exposed to calcein-AM. Calcein-AM is rapidly taken up by cells and deesterified by endogeneous esterases, resulting in the accumulation of calcein within the cells. If Pgp is

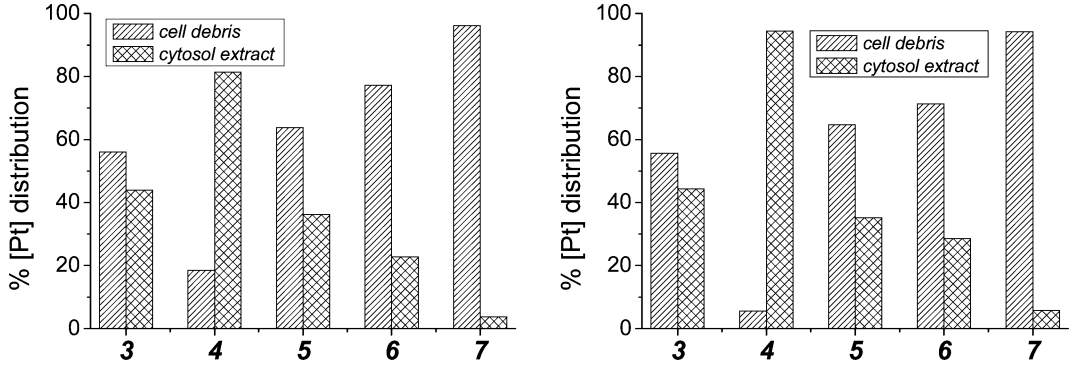

Figure 6. Distribution between cytosol and membrane fraction of complexes **3**−**7** in A549 lung carcinoma cells (left) and HT29 colon carcinoma cells (right). Cells were grown to confluence, and then fresh medium containing drugs at 1 μM was added for 24 h. The cytosol and cell debris fractions were separated, and Pt levels were separately quantified using ICP-MS.

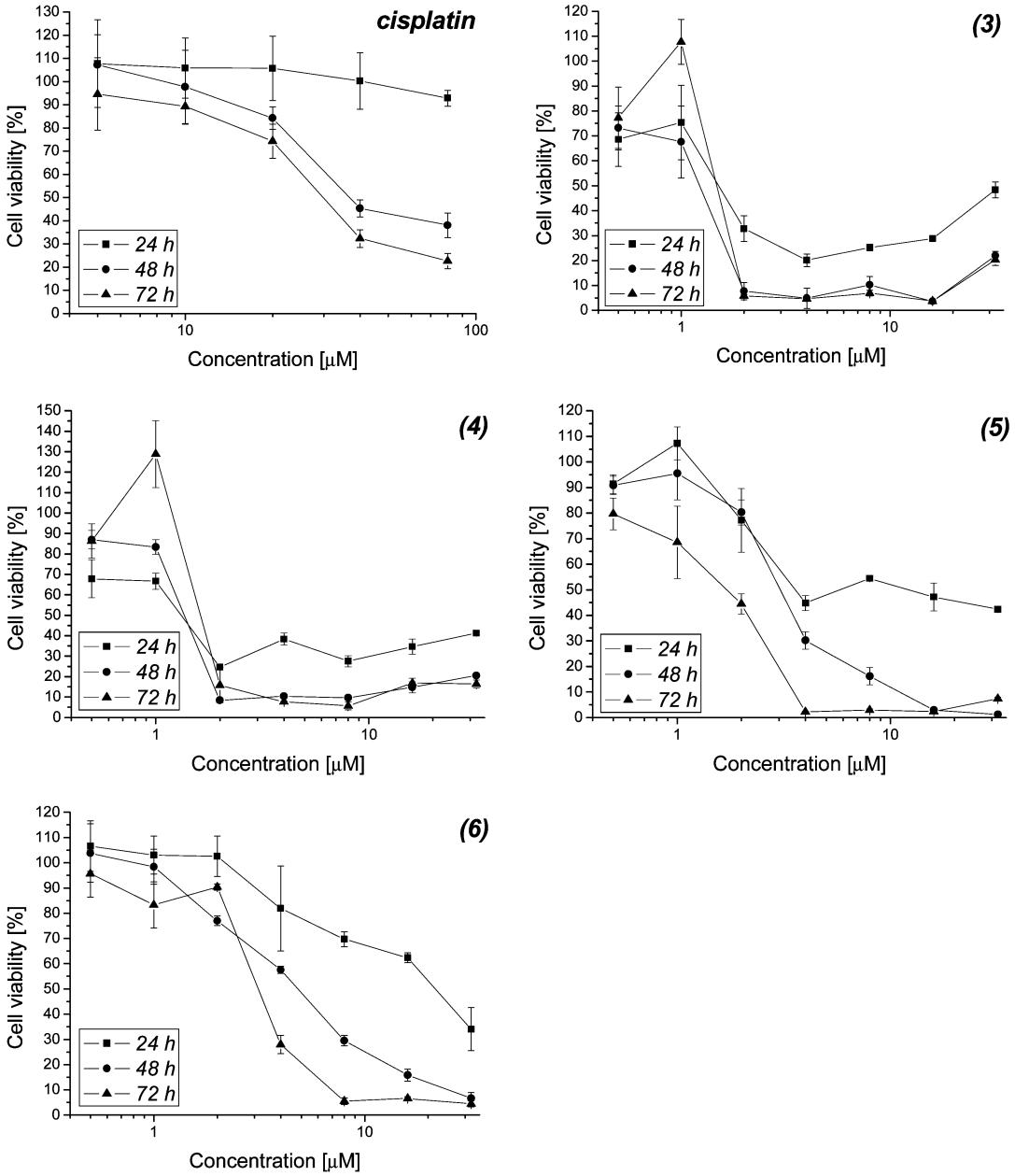

Figure 7. Time-dependent and dose-dependent drug efficacy studies for cisplatin and complexes **3**−**6** on A549 lung carcinoma cells. Cells were grown to confluence, then fresh medium containing drugs at increasing concentrations was added for 24, 48, or 72 h, and MTT test was performed for the last 2 h.

present in the cells, calcein is rapidly expelled, and the process may be blocked using Pgp inhibitors such as verapamil. A dose−response relationship between cellular calcein levels and verapamil was observed in A549

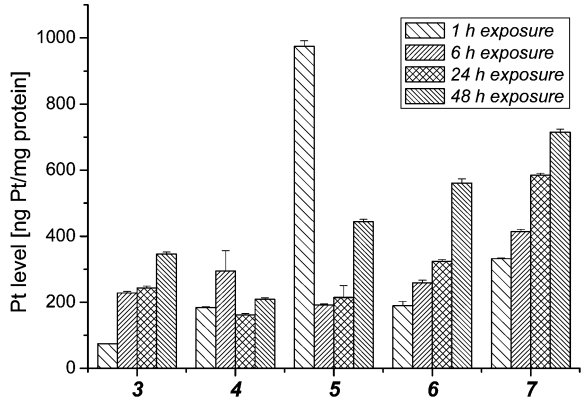

Figure 8. Uptake of complexes **3**−**7** by A549 lung carcinoma cells in combination with the Pgp-inhibitor, verapamil. Cells were grown to confluence, then fresh medium containing drugs at 1 μM and verapamil at 100 μM was added for 1, 6, 24, or 48 h. Pt levels of harvested cells were quantified using ICP-MS.

and HT29 cells (Figure S-2), indicating the presence of Pgp. To examine the effect of Pgp-induced drug efflux of the complexes, A549 cells were exposed continuously to both verapamil (100 μM) and drugs (1 μM) for 1, 6, 24, and 48 h, and the Pt levels were quantified using ICP-MS (Figure 8). A distinct change in the uptake profile was observed, with Pt levels increasing gradually over time, particularly in cells treated with complex **7**. This suggests that the efflux of the Pt complexes tested, mediated in part by Pgp, may be involved in resistance to growth inhibition by the Pt(IV) aryl carboxylates.

The cell-growth inhibition efficacy of the complexes against A549 cells were studied in combination with verapamil. As expected, cisplatin and complexes **2** and **8** remained ineffective up to 80 μM within 24 h because their low efficacies were hypothesized to result from poor uptake rather than drug efflux. No significant enhancement in drug efficacy for complexes **3**−**6** was observed, which corresponds to the observation that Pt levels remain largely unchanged, within 150−300 ng Pt/mg protein with or without verapamil co-treatment, in these complexes. This could be due to the lower efficiency of efflux mechanisms as compared to that of uptake within 24 h of drug exposure. However, for complex **7**, significant enhancement (Figure 9) in drug efficacy was observed, although not reaching the levels achieved by complexes **3**−**6**. This suggests that MDR pathways are involved in the efflux of complex **7**, possibly because it is a better substrate for Pgp and could, therefore, be more effectively expelled from the cells, and at least partly responsible for its lower-than-expected drug efficacy.

Conclusions

trans-Pt(IV) aryl carboxylate complexes are attractive scaffolds to build specific functionalities, which could be used to achieve desirable pharmacological attributes, and our results clearly demonstrate that the functionalization of the aromatic carboxylate ligand strongly influences drug activities of this class of complex. A close correlation between drug uptake and efficacy in the complexes tested suggests drug uptake as an important factor in determining their effectiveness as human tumor cell-growth inhibitors. The highly efficacious **3**, **4**, **5**, and **6** were found to accumulate strongly in the cells, with **4** showing highest levels of penetration into the cytosol. In contrast, the cyano group dramatically reduces drug efficacy. Pgp-mediated drug efflux mechanisms are also evidently involved in the decreased efficacy of some complexes, such as **7**. The carboxylic acid functionality that could deprotonate at biological pH, e.g., in complex **8**, was also found to be unfavorable as it resulted in poor drug uptake. The results of the study could have implications on future Pt drug design, including the development of drugs for specific drug targets, both intracellular and extracellular.

Experimental Section

All reagents were purchased from Acros Chemicals unless otherwise indicated. K_2PtCl_4 was obtained from Precious Metals Online. 4-Iodobenzoyl chloride was purchased from Lancaster Synthesis, Calcein-AM, benzoyl chloride, and 4-methoxybenzoyl chloride from Fluka, and phthalic anhydride and acetic anhydride from Aldrich. The reactions were performed with solvents dried using appropriate reagents and distilled prior to use. *cis*,*cis*,*trans*-Diamminedichlorodihydroxylplatinum-(IV) **1**, 4-vinylbenzoic acid, and 4-vinylbenzoyl chloride were prepared and purified according to literature procedures.[30,31] IR spectra were recorded on a Perkin-Elmer FT-IR 2000 system. NMR spectra were measured on a Bruker DMX 400, using $SiMe_4$ for ^1H and ^{13}C and Na_2PtCl_6 for ^{195}Pt as external standards at 20 °C. Negative mode nanospray ionization mass spectra (NSI-MS) for synthesized compounds were recorded

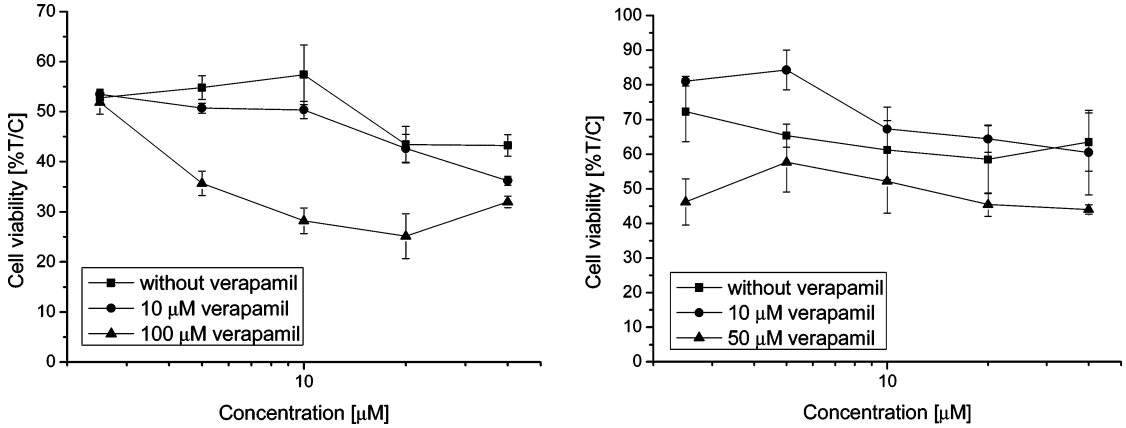

Figure 9. Increased efficacy of complex **7** in A549 (left) and HT29 (right) in the presence of the Pgp-inhibitor verapamil. Cells were grown to confluence, then fresh medium containing **7** at increasing concentrations and verapamil at 10 μM, 50 μM, or 100 μM was added for 24 h. MTT assay was performed for the last 2 h.

on a ThermoFinnigan LCQ Deca XP Plus quadrupole ion trap instrument on samples dissolved in methanol with ionization energy set as 1.5 V and capillary temperature at 150 °C, as previously described.[21] Elemental analyses were carried out at the Institute of Chemical Sciences and Engineering (EPFL).

Synthesis of $Pt(NH_3)_2Cl_2(CO_2CH_3)_2$, 2. The synthetic procedure used was adapted from literature.[32] A suspension of **1** (154 mg, 0.46 mmol) in acetic anhydride (20 mL) was stirred under nitrogen over a period of 5 days. Hexane (20 mL) was added to precipitate the product, which was filtered and washed with diethyl ether. The product mixture was extracted with THF (10 mL), leaving small amounts of unreacted starting material. The solvent was removed in vacuo, and the residue was redissolved in THF (10 mL) and precipitated from pentane (40 mL) to yield a pale yellow powder. The product was dried in vacuo (yield: 67 mg, 35%). Anal. ($C_4H_{12}Cl_2N_2O_4Pt$) C, H, N.

Synthesis of $Pt(NH_3)_2Cl_2(CO_2C_6H_5)_2$, 3. Benzoyl chloride (0.9 mL, 7.81 mmol) in acetone (5 mL) was added dropwise to a mixture of pyridine (1.0 mL, 12.38 mmol) and **1** (99 mg, 0.30 mmol) in acetone (3 mL). The mixture was brought to reflux and maintained at 75 °C for 4 h. Excess hexane (10 mL) was added, and the reaction mixture was filtered. The filtered precipitate was triturated in diethyl ether (20 mL), filtered, and washed with water to remove the pyridinium salt. The residue was redissolved in THF (5 mL) and precipitated from pentane (20 mL) to yield a pale yellow powder. The product was dried in vacuo (yield: 48 mg, 30%). Crystals suitable for X-ray diffraction were grown from vapor diffusion of pentane into a solution of **3** in THF. ^{1}H NMR (THF-d_8, 400.13 MHz): 8.05 (d, 4H, *o*-Ar−H, $^3J_{HH}$ = 7.6 Hz), 7.44 (d, 2H, *p*-Ar−H, $^3J_{HH}$ = 7.2 Hz), 7.34 (dd, 4H, *m*-Ar−H, $^3J_{HH}$ = 7.2, 7.6 Hz), 6.41 (m, 6H, NH_3, $^1J_{HN}$ = 53.4 Hz, $^2J_{HPt}$ = 56.3 Hz). ^{13}C−{^{1}H} NMR (THF-d_8, 100.61 MHz): 175.0 (−CO_2−), 134.2, 132.3, 130.8, 128.5 (Ar−C). ^{195}Pt−{^{1}H} NMR (THF-d_8, 86.13 MHz): 1076.63 ppm (q, $^1J_{PtN}$ = 176 Hz). ESI-MS (MeOH, -ve mode) *m/z*: 541.3 [M − H]$^-$, 1118.7 [M_2 − H]$^-$, 1660.1 [M_3 − H]$^-$, Anal. ($C_{14}H_{16}Cl_2N_2O_4Pt$·0.5THF) C, H, N.

Synthesis of $Pt(NH_3)_2Cl_2(CO_2C_6H_4CH{=}CH_2)_2$, 4. The compound was synthesized in accordance to the method used for compound **3** (yield: 18 mg, 67%). Crystals suitable for X-ray diffraction were grown from vapor diffusion of pentane into a solution of **4** in THF. ^{1}H NMR (THF-d_8, 400.13 MHz): 8.01 (d, 4H, Ar−H, $^3J_{HH}$ = 8.0 Hz), 7.42 (d, 4H, Ar−*H*, $^3J_{HH}$ = 8.0 Hz), 6.77 (dd, 2H, −C*H*=C, $^3J_{HH}$ = 11.2, 17.6 Hz), 6.49 (m, 6H, N*H*$_3$, $^1J_{HN}$ = 53.4 Hz, $^2J_{HPt}$ = 52.9 Hz), 5.87 (d, 2H, −C=C*H*, $^3J_{HH}$ = 17.6 Hz), 5.29 (d, 2H, −C=C*H*, $^3J_{HH}$ = 11.2 Hz). ^{13}C−{^{1}H} NMR (THF-d_8, 100.61 MHz): 175.1 (−CO_2−), 141.9, 133.8, 131.4, 126.7 (Ar−*C*), 137.9 (−*C*H=C), 115.9 (−C=*C*H$_2$). ^{195}Pt−{^{1}H} NMR (THF-d_8, 86.01 MHz): 1077.80 ppm (q, $^1J_{PtN}$ = 172 Hz). ESI-MS (MeOH, -ve mode) *m/z*: 590.9 [M − H]$^-$, 1186.1 [M_2 − H]$^-$, Anal. ($C_{18}H_{20}Cl_2N_2O_4Pt$) C, H, N.

Synthesis of $Pt(NH_3)_2Cl_2(CO_2C_6H_4OCH_3)_2$, 5. Anisoyl chloride (0.43 g, 3.32 mmol) in acetone (5 mL) was added dropwise to a mixture of pyridine (0.5 mL, 6.19 mmol) and **1** (49 mg, 0.15 mmol) in acetone (3 mL). The mixture was brought to reflux and maintained at 75 °C overnight. The reaction mixture was concentrated under vacuum, then water (20 mL) was added to quench the reaction, and the mixture was left at 2 °C for 8 h. The precipitate was filtered, washed with water, triturated in diethyl ether (20 mL), and filtered. The residue was redissolved in THF (5 mL) and precipitated from pentane (20 mL) to yield a pale yellow powder. The product was dried in vacuo (yield: 46 mg, 52%). ^{1}H NMR (THF-d_8, 400.13 MHz): 8.00 (d, 4H, Ar−*H*, $^3J_{HH}$ = 7.9 Hz), 6.85 (d, 4H, Ar−*H*, $^3J_{HH}$ = 7.9 Hz), 6.42 (m, 6H, N*H*$_3$, $^1J_{HN}$ = 53.2 Hz, $^2J_{HPt}$ = 52.8 Hz), 3.81 (s, 3H, −C*H*$_3$). ^{13}C−{^{1}H} NMR (THF-d_8, 100.61 MHz): 175.0 (−CO_2−), 163.6, 131.3, 113.6 (Ar−*C*), 55.6 (−O*C*H$_3$). ^{195}Pt−{^{1}H} NMR (THF-d_8, 86.01 MHz): 1083.41 ppm (q, $^1J_{PtN}$ = 179 Hz). ESI-MS (MeOH, -ve mode) *m/z*: 601.3 [M − H]$^-$, 664.1 [M − H + 2(MeOH)]$^-$, 1265.5 [M_2 − H + 2(MeOH)]$^-$. Anal. ($C_{16}H_{20}Cl_2N_2O_6Pt$·H_2O) C, H, N: calcd, 4.52; found, 4.09.

Synthesis of $Pt(NH_3)_2Cl_2(CO_2C_6H_4I)_2$, 6. 4-Iodobenzoyl chloride (800 mg, 3.00 mmol) in acetone (10 mL) was added dropwise to a mixture of pyridine (1.0 mL, 12.26 mmol) and **1** (205 mg, 0.62 mmol) in acetone (5 mL). The mixture was brought to reflux and maintained at 75 °C for 4 h. Water (30 mL) was added to quench the reaction, and the product mixture was chilled at 2 °C overnight. The precipitate formed was filtered, washed with water, triturated in diethyl ether (50 mL), and filtered. Boiling toluene (100 mL) was added to extract 4-iodobenzoic acid to yield a pale brown powder. The product was dried in vacuo (yield: 382 mg, 78%). ^{1}H NMR (THF-d_8, 400.13 MHz): 7.76 (dd, 8H, Ar−*H*, $^3J_{HH}$ = 8.7 Hz), 6.37 (m, 6H, N*H*$_3$, $^1J_{HN}$ = 53.5 Hz, $^2J_{HPt}$ = 52.0 Hz). ^{13}C−{^{1}H} NMR (DMSO-d_6, 100.61 MHz): 172.6 (−CO_2−), 137.4, 132.5, 131.3, 99.7 (Ar−*C*). ^{195}Pt−{^{1}H} NMR (THF-d_8, 86.01 MHz): 1074.82 ppm (q, $^1J_{PtN}$ = 173 Hz). ESI-MS (MeOH, -ve mode) *m/z*: 792.7 [M − H]$^-$, Anal. ($C_{14}H_{14}Cl_2I_2N_2O_4Pt$·0.2toluene) C, H, N.

Synthesis of $Pt(NH_3)_2Cl_2(CO_2C_6H_4CN)_2$, 7. 4-Cyanobenzoyl chloride (600 mg, 3.55 mmol) in acetone (5 mL) was added dropwise to a mixture of pyridine (5 mL, 61.88 mmol) and **1** (98 mg, 0.29 mmol) in acetone (3 mL). The mixture was brought to reflux and maintained at 75 °C overnight. The reaction mixture was concentrated under a rotavap, then water (20 mL) was added to quench the reaction, and the product mixture was chilled at 2 °C for 8 h. The precipitate was filtered, washed with water, triturated in diethyl ether (30 mL), and filtered. Cold THF (10 mL) added to extract 4-cyanobenzoic acid from the product mixture, and the residue was redissolved in hot THF (10 mL) and precipitated from pentane (40 mL) to yield a white powder. The product was dried in vacuo (yield: 50 mg, 28%). Crystals suitable for X-ray diffraction were grown from vapor diffusion of pentane into a solution of **7** in THF. ^{1}H NMR (THF-d_8, 400.13 MHz): 8.18 (d, 4H, Ar−*H*, $^3J_{HH}$ = 8.8 Hz), 7.75 (d, 4H, Ar−*H*, $^3J_{HH}$ = 8.8 Hz), 6.37 (m, 6H, N*H*$_3$, $^1J_{HN}$ = 53.2 Hz, $^2J_{HPt}$ = 53.6 Hz). ^{13}C−{^{1}H} NMR (DMSO-d_6, 100.61 MHz): 171.5 (−CO_2−), 136.9, 132.2, 129.7, 113.9 (Ar−*C*), 118.4 (−*C*N). ^{195}Pt−{^{1}H} NMR (THF-d_8, 86.01 MHz): 1067.47 ppm (q, $^1J_{PtN}$ = 167 Hz). ESI-MS (MeOH, -ve mode) *m/z*: 626.7 [M + 2H_2O − H]$^-$, 610.1 [M + H_2O − H]$^-$, 591.1 [M − H]$^-$. Anal. ($C_{16}H_{14}Cl_2N_4O_4Pt$·0.5H_2O) C, H, N.

Synthesis of $Pt(NH_3)_2Cl_2(CO_2C_6H_4COOH)_2$, 8. Phthalic anhydride (95 mg, 6.35 mmol) was added to a mixture of **1** (99 mg, 0.30 mmol) in DMSO (10 mL). The reaction mixture was stirred at 80 °C for 6 h, during which the starting material dissolved to form a yellow solution. Water (20 mL) was added to quench the reaction, and the product mixture was stored at 2 °C overnight. The precipitate obtained was filtered, washed with water, triturated in diethyl ether (10 mL), and filtered. The residue was redissolved in THF (5 mL) and precipitated from pentane (20 mL) to yield a pale yellow powder. The product was dried in vacuo (yield: 99 mg, 53%). Crystals suitable for X-ray diffraction were grown from vapor diffusion of pentane into a solution of **8** in THF. ^{1}H NMR (THF-d_8, 400.13 MHz): 11.90 (br, 2H, CO_2H), 7.80 (d, 2H, Ar−*H*, $^3J_{HH}$ = 8.8 Hz), 7.55 (d, 2H, Ar−*H*, $^3J_{HH}$ = 22.4 Hz), 6.36 (m, 6H, N*H*$_3$, $^1J_{HN}$ = 52.8 Hz, $^2J_{HPt}$ = 53.6 Hz). ^{13}C −^{1}H} NMR (THF-d_6, 100.61 MHz): 177.4 (−CO_2−), 169.4 (−CO_2H), 137.5, 132.0, 131.4, 130.0, 129.7, 128.9 (Ar−*C*). ^{195}Pt−{^{1}H} NMR (THF-d_8, 86.01 MHz): 1087.17 ppm (q, $^1J_{PtN}$ = 173 Hz). ESI-MS (MeOH, -ve mode) *m/z*: 1259.1 [M_2 − H]$^-$, 629.3 [M − H]$^-$, Anal. ($C_{16}H_{14}Cl_2N_4O_4Pt$·THF) C, N, H: calcd, 3.44; found, 3.85

Structural Characterization of Complexes 3, 4, 7, and 8 in the Solid State. Relevant details about the structure refinements are compiled in Table 1 and selected bond distances and angles given in the captions of Figure 4a−d and Table S3. Data collection for the X-ray structure determinations for complexes **4**, **7**, and **8** were performed on a four-circle Kappa goniometer equipped with an Oxford Diffraction KM4 Sapphire CCD at 140(2) K, whereas data for complex **3** was collected on a mar345 IPDS instrument at 140(2) K. Data reduction was performed using CrysAlis RED.[33] Structure solutions were performed for complexes **4** and **8** using SHELX-TL software package for all compounds[34] and for complexes **3**

and **7** using SiR97.[35] Structures were solved by full-matrix least-squares refinement (against F^2) with all non-hydrogen atoms refined anisotropically. Hydrogen atoms were placed in their geometrically generated positions and refined using the riding model. For complex **4**, disorder for the solvated THF molecules was modeled. Empirical absorption corrections (DELABS) were applied for all of the structures.[36] Graphical representations of the structures were made with Ortep-3.[37]

Cell Culture. Human T47D and MCF-7 breast carcinoma, A549 lung carcinoma, and HT-29 colon carcinoma cell lines were obtained from the American Type Culture Collection (ATCC, Manassas, VA). All other cell culture reagents were obtained from Gibco-BRL, Basel, Switzerland. The cells were routinely grown in DMEM medium containing 4.5 g/L glucose, 10% foetal calf serum (FCS), and antibiotics at 37 °C and 6% CO_2. For the MTT tests, the cells were seeded in 48-well plates (Costar, Integra Biosciences, Cambridge, MA) as monolayers for 24−48 h in complete medium to reach confluence; then fresh complete medium was added together with the drugs, and culture was continued for another 24−72 h. The test (see below) was performed for the last 2 h without changing the culture medium. For the determination of Pt uptake, the cells were subcultured in 12-well plates (Costar) (10^6 cells/well at confluence) 48 h prior to incubation with the test compounds.

Determination of Protein Concentration. Protein content was determined with the BCA protein assay kit (Pierce, Socachim, Switzerland) using bovine serum albumin as the standard, according to the procedure recommended by the manufacturer.

Determination of Cell Viability. The compounds were predissolved in DMSO (10 mM) and diluted with cell culture medium to the required concentration, such that the total DMSO concentration did not exceed 0.8%. At this concentration, DMSO was found to be nontoxic to the cells tested. Verapamil (Isoptin for injection, 2.5 mg per mL PBS, Abbott) was added directly to the cell culture medium to the required concentration before the addition of the test compounds, for the experiments requiring co-treatment. The cells were exposed to the drugs for the required length of time. Cell viability was determined using the MTT assay, which allows the quantification of the mitochondrial activity in metabolically active cells. Following drug exposure, MTT (final concentration 0.2 mg/mL) was added to the cells for 2 h; then the culture medium was aspirated, and the violet formazan precipitate was dissolved in 0.1 N HCl in 2-propanol. The optical density, which is directly proportional to the number of surviving cells, was quantified at 540 nm using a multiwell plate reader (iEMS Reader MF, Labsystems, U.S.A.), and the fraction of surviving cells was calculated from the absorbance of untreated control cells.[25]

Determination of Intracellular Pt Level. The test compounds were predissolved in DMSO (10 mM) and diluted with cell culture medium to either 10 or 1 μM. Verapamil was added directly to the cell culture medium to the required concentration before the addition of the test compounds. The cells were exposed continuously to the drugs for the required length of time at 37 °C in standard culture conditions, washed three times with sterile phosphate buffered saline (PBS), and then treated with sodium acetate buffer (150 μM, pH 5.2) for 10 min to remove any nonspecific interactions and washed again with PBS. The cells were harvested by trypsinization, concentrated by centrifugation at 1000 g, and diluted to 1 mL with sterile PBS. The cells were homogenized in an ultrasound bath for 15 min before determining the protein content. Thereafter, the cells were mineralized in boiling 65% v/w HNO_3 (Merck P. A. grade), and the Pt levels were determined using ICP-MS as an aqueous solution in 1% v/w HNO_3 in Nanopure water (R > 18.2 Ω). To extract the cytosol, the cells were centrifuged at 15 000*g* for 20 min, after homogenization in an ultrasound bath, and the supernatant was carefully separated from the resulting cell debris. The supernatant layer was dried in vacuo and redissolved in 1% v/w HNO_3 solution. The cell debris was mineralized in boiling HNO_3 and treated as before.

ICP-MS Measurements. Platinum levels were quantified using a Perkin-Elmer Elan 6100 DRC Inductively Coupled Plasma-Mass Spectrometer. Instrumental settings were optimized to yield maximum sensitivity for platinum. The most abundant isotopes of platinum were measured at *m/z* 194 and 195. The raw counts for Pt 194 or 195 were over 8000 counts per second (cps) for 1 μg/L Pt solution, and the background was below 10 cps. Rhodium was used as an internal standard, measured at *m/z* 103. The sample solutions were prepared by dissolving dried platinum-containing materials in 1% v/w HNO_3 in Nanopure water (R > 18.2 Ω), with 50 μg/L of rhodium standard. ICP-MS standard, chemical blank, and 1 μg/L Pt internal monitor solutions were made following the same procedure. The calibration curve was calculated using five standard solutions (1, 10, 100, 500, and 1000 μg/L of platinum) after chemical blank subtraction. Concentration values were corrected with respect to the rhodium signal. Pt internal monitor solution (1 μg/L) was measured as an unknown sample every 8−12 analyses to control the ICP-MS drift during the measurements. Platinum concentration in Nanopure water and chemical blank was below 1 μg/mL and 0.3 μg/L, respectively.

Calcein Uptake Assay. The Pgp activity of HT29 colon carcinoma and A549 lung carcinoma was evaluated by calcein-AM (Fluka) uptake assay in the method described by Weiss et al.[29] The assay was performed on cells seeded on 48-well plates. Prior to the assay, the cells were washed twice with prewarmed Hanks balanced salt solution supplemented with 10 mM HEPES (HHBSS) and preincubated with HHBSS for 30 min and then with Verapamil for 15 min. Calcein-AM, predissolved in dry DMSO, was then added (to reach a final concentration of 1 μM), and the cells were incubated for a further 60 min. The uptake was stopped by transferring the plates onto ice, and the cells were washed twice with chilled HHBSS. The cells were then lysed in 1% Triton X-100/PBS for 15 min, and the fluorescence of the calcein generated was analyzed in a multiwell fluorometric plate reader, λ_{ex} = 485 nm excitation and λ_{em} = 530 filters (PerSeptive, Biosystems, MA).

Acknowledgment. We thank the Roche Research Foundation (W.H.A.) and Swiss Cancer League (P.J.D., L.J.J.) for financial support. We also thank Dr Heinz Rüegger (ETHZ) and Dr Tilmann Gelbach (EPFL) for their useful discussions regarding the NMR spectra.

Supporting Information Available: Spectroscopic and elemental analysis data of the target compounds. Crystallographic information of **3**, **4**, **7**, and **8** in CIF format, Figures S-1 and S-2, Tables S-1, S-2, S-3, and S-4. This material is available free of charge via the Internet at http://pubs.acs.org.

References

(1) Boulikas, T.; Vougiouka, M. Cisplatin and Platinum Drugs at the Molecular Level (Review). *Oncol. Rep.* **2003**, *10*, 1663−1682; Agarwal, R.; Kaye, S. B. Ovarian Cancer: Strategies for Overcoming Resistance to Chemotherapy. *Nat. Rev. Cancer* **2003**, *3*, 502−516.

(2) Pasini, A.; Zunino, F. New Cisplatin Analogs − On the Way to Better Antitumor Agents. *Angew. Chem., Int. Ed. Engl.* **1987**, *26*, 615−624; Galanski, M.; Arion, V. B.; Jakupec, M. A.; Keppler, B. K. Recent Developments in the Field of Tumor-Inhibiting Metal Complexes. *Curr. Pharm. Des.* **2003**, *9*, 2078−2089; Wong, E.; Giandomenico, C. M. Current Status of Platinum-Based Antitumor Drugs. *Chem. Rev.* **1999**, *99*, 2451−2466.

(3) Fuertes, M. A.; Castilla, J.; Alonson, C.; Perez, J. M. Novel Concepts in the Development of Platinum Antitumour Drugs. *Curr. Med. Chem.: Anti-Cancer Agents* **2002**, *2*, 539−551.

(4) Fuertes, M. A.; Alonso, C.; Perez, J. M. Biochemical Modulation of Cisplatin Mechanisms of Action: Enhancement of Antitumor Activity and Circumvention of Drug Resistance. *Chem. Rev.* **2003**, *103*, 645−662.

(5) Sundquist, W. I.; Lippard, S. J. The Coordination Chemistry of Platinum Anticancer Drugs and Related-Compounds with DNA. *Coord. Chem. Rev.* **1990**, *100*, 293−322.

(6) Raymond, E.; Faivre, S.; Chaney, S.; Woynarowski, J.; Cvitkovic, E. Cellular and Molecular Pharmacology of Oxaliplatin. *Mol. Cancer Ther.* **2002**, *1*, 227−235.

(7) Lee, Y. A.; Chung, Y. K.; Sohn, Y. S. Synthesis and Antitumor Activity of (Diamine)platinum(II) Complexes of Benzylmalonate Derivatives. *J. Inorg. Biochem.* **1997**, *68*, 289−294; Hasinoff, B. B.; Wu, X.; Yang, Y. W. Synthesis and Characterization of the Biological Activity of the Cisplatin Analogues, *cis*-$PtCl_2$(dexrazoxane) and *cis*-$PtCl_2$(levrazoxane), of the Topoisomerase II Inhibitors Dexrazoxane (ICRF-187) and Levrazoxane (ICRF-186). *J. Inorg. Biochem.* **2004**, *98*, 616−624; Galanski, M.; Slaby, S.; Jakupec, M. A.; Keppler, B. K. Synthesis, Characterization, and in vitro Antitumor Activity of Osteotropic Diam(m)ineplatinum(II) Complexes Bearing a *N*,*N*-bis(phosphonomethyl)glycine Ligand. *J. Med. Chem.* **2003**, *46*, 4946−4951; Descôteaux, C.; Provencher-Mandeville, J.; Mathieu, I.; Perron, V.; Asselin, E.; Bérube, G.; Mandal, S. K. Synthesis of 17β-estradiol Platinum-(II) Complexes: Biological Evaluation on Breast Cancer Cell Lines. *Bioorg. Med. Chem. Lett.* **2003**, *13*, 3927−3931.

(8) Cleare, M. J.; Hoeschele, J. D. Studies on the Antitumor Activity of Group VIII Transition Metal Complexes. Part I. Platinum (II) Complexes. *Bioinorg. Chem.* **1973**, *2*, 187−210.

(9) Barnes, K. R.; Kutikov, A.; Lippard, S. J. Synthesis, Characterization, and Cytotoxicity of a Series of Estrogen-Tethered Platinum(IV) Complexes. *Chem. Biol.* **2004**, *11*, 557−564.

(10) Ang, W. H.; Khalaila, I.; Allardyce, C. S.; Juillerat-Jeanneret, L.; Dyson, P. J. Rational Design of Platinum(IV) Compounds to Overcome Glutathione-S-transferase Mediated Drug Resistance. *J. Am. Chem. Soc.* **2005**, *127*, 1382−1383.

(11) Hall, M. D.; Hambley, T. W. Platinum(IV) Antitumour Compounds: Their Bioinorganic Chemistry. *Coord. Chem. Rev.* **2002**, *232*, 49−67.

(12) Sternberg, C. N.; Whelan, P.; Hetherington, J.; Paluchowska, B.; Slee, P. H. T. J.; Vekemans, K.; Van Erps, P.; Theodore, C.; Koriakine, O.; Oliver, T.; Lebwohl, D.; Debois, M.; Zurlo, A.; Collette, L. Phase III Trial of Satraplatin, An Oral Platinum Plus Prednisone vs Prednisone Alone in Patients with Hormone-Refractory Prostate Cancer. *Oncology* **2005**, *68*, 2−9; Vouillamoz-Lorenz, S.; Buclin, T.; Lejeune, F.; Bauer, J.; Leyvraz, S.; Decosterd, L. A. Pharmacokinetics of Satraplatin (JM216), An Oral Platinum(IV) Complex under Daily Oral Administration for 5 or 14 Days. *Anticancer Res.* **2003**, *23*, 2757−2765.

(13) Hanessian, S.; Zhan, L. J.; Bovey, R.; Saavedra, O. M.; Juillerat-Jeanneret, L. Functionalized Glycomers as Growth Inhibitors and Inducers of Apoptosis in Human Glioblastoma Cells. *J. Med. Chem.* **2003**, *46*, 3600−3611.

(14) Fiaux, H.; Popowycz, F.; Favre, S.; Schütz, C.; Vogel, P.; Gerber-Lemaire, S.; Juillerat-Jeanneret, L. Functionalized Pyrrolidines Inhibit α-Mannosidase Activity and Growth of Human Glioblastoma and Melanoma Cells. *J. Med. Chem.* **2005**, *48*, 4237−4246.

(15) Giandomenico, C. M.; Abrams, M. J.; Murrer, B. A.; Vollano, J. F.; Rheinheimer, M. I.; Wyer, S. B.; Bossard, G. E.; Higgins, J. D. Carboxylation of Kinetically Inert Platinum(IV) Hydroxyl Complexes − An Entree into Orally Active Platinum(IV) Antitumor Agents. *Inorg. Chem.* **1995**, *34*, 1015−1021.

(16) Galanski, M.; Keppler, B. K. Carboxylation of Dihydroxoplatinum(IV) Complexes via a New Synthetic Pathway. *Inorg. Chem.* **1996**, *35*, 1709−1711.

(17) Kelland, L. R.; Murrer, B. A.; Abel, G.; Giandomenico, C. M.; Mistry, P.; Harrap, K. R. Ammine Amine Platinum(IV) Dicarboxylates − A Novel Class of Platinum Complex Exhibiting Selective Cytotoxicity to Intrinsically Cisplatin-Resistant Human Ovarian-Carcinoma Cell-Lines. *Cancer Res.* **1992**, *52*, 822−828; Kelland, L. R.; Mistry, P.; Abel, G.; Loh, S. Y.; Oneill, C. F.; Murrer, B. A.; Harrap, K. R. Mechanism-Related Circumvention of Acquired cis-Diamminedichloroplatinum(II) Resistance using 2 Pairs of Human Ovarian-Carcinoma Cell-Lines by Ammine Amine Platinum(IV) Dicarboxylates. *Cancer Res.* **1992**, *52*, 3857−3864.

(18) Ormerod, M. G.; Orr, R. M.; ONeill, C. F.; Chwalinski, T.; Titley, J. C.; Kelland, L. R.; Harrap, K. R. The Cytotoxic Action of Four Ammine/Amine Platinum(IV) Dicarboxylates: A Flow Cytometric Study. *Br. J. Cancer* **1996**, *74*, 1935−1943.

(19) Kim, K. M.; Lee, Y.-A.; Lee, S. S.; Sohn, Y. S. Facile Synthesis and Structural Properties of (Diamine)tetracarboxylatoplatinum-(IV) Complexes. *Inorg. Chim. Acta* **1999**, *292*, 52−56.

(20) Song, R.; Kim, K. M.; Lee, S. S.; Sohn, Y. S. Electrophilic Substitution of (Diamine)tetrahydroxoplatinum(IV) with Carboxylic Anhydrides. Synthesis and Characterization of (Diamine)platinum(IV) Complexes of Mixed Carboxylates. *Inorg. Chem.* **2000**, *39*, 3567−3571.

(21) Dyson, P. J.; McIndoe, J. S. Analysis of Organometallic Compounds using Ion Trap Mass Spectrometry. *Inorg. Chim. Acta* **2003**, *354*, 68−74.

(22) Heinz, R. Personal communication.

(23) Galanski, M.; Keppler, B. K. Carboxylation of Dihydroxoplatinum(IV) Complexes with Acyl Chlorides. Crystal Structures of the *trans-R*, *R*- and *trans-S*, *S*-isomer of (OC-6−33)-bis(1-adamantanecarboxylato)−(cyclohexane-1,2-diamine)dichloroplatinum(IV). *Inorg. Chim. Acta* **1997**, *265*, 271−274; Neidle, S.; Snook, C. F.; Murrer, B. A.; Barnard, C. F. J. Bis(acetato)-amminedichloro(cyclohexylamine)platinum(IV), an Orally Active Anticancer Drug. *Acta Crystallogr., Sect. C: Cryst. Struct. Commun.* **1995**, *51*, 822−824.

(24) Kwon, Y. E.; Whang, K. J.; Park, Y. J.; Kim, K. H. Synthesis, Characterization and Antitumor Activity of Novel Octahedral Pt(IV) Complexes. *Bioorg. Med. Chem.* **2003**, *11*, 1669−1676; Song, R.; Park, S. Y.; Kim, Y.-S.; Kim, Y.; Kim, S.-J.; Ahn, B. T.; Sohn, Y. S. Synthesis and Cytotoxicity of New Platinum(IV) Complexes of Mixed Carboxylates. *J. Inorg. Biochem.* **2003**, *96*, 339−345.

(25) Mosmann, T. Rapid Colorimetric Assay for Cellular Growth and Survival − Application to Proliferation and Cytotoxicity Assays. *J. Immunol. Methods* **1983**, *65*, 55−63.

(26) Hambley, T. W.; Battle, A. R.; Deacon, G. B.; Lawrenz, E. T.; Fallon, G. D.; Gatehouse, B. M.; Webster, L. K.; Rainone, S. Modifying the Properties of Platinum(IV) Complexes in order to Increase Biological Effectiveness. *J. Inorg. Biochem.* **1999**, *77*, 3−12; Hall, M. D.; Amjadi, S.; Zhang, M.; Beale, P. J.; Hambley, T. W. The Mechanism of Action of Platinum(IV) Complexes in Ovarian Cancer Cell Lines. *J. Inorg. Biochem.* **2004**, *98*, 1614−1624; Battle, A. R.; Deacon, G. B.; Dolman, R. C.; Hambley, T. W. Electrochemistry, Protein Binding and Crystal Structures of Platinum(II) and Platinum(IV) Carboxylato Complexes. *Aust. J. Chem.* **2002**, *55*, 699−704.

(27) Leo, A.; Hansch, C.; Elkins, D. Partition Coefficients and Their Uses. *Chem. Rev.* **1971**, *71*, 525−616.

(28) Ghezzi, A.; Aceto, M.; Cassino, C.; Gabano, E.; Osella, D. Uptake of Antitumor Platinum(II)-Complexes by Cancer Cells, Assayed by Inductively Coupled Plasma Mass Spectrometry (ICP-MS). *J. Inorg. Biochem.* **2004**, *98*, 73−78.

(29) Weiss, J.; Dormann, G.; Martin-Facklam, M.; Kerpen, C. J.; Ketabi-Kiyanvash, N.; Haefeli, W. E. Inhibition of P-glycoprotein by Newer Antidepressants. *J. Pharmacol. Exp. Ther.* **2003**, *305*, 197−204.

(30) Brandon, R. J.; Dabrowiak, J. C. Synthesis, Characterization, and Properties of a Group of Platinum(IV) Complexes. *J. Med. Chem.* **1984**, *27*, 861−865.

(31) Cameron, J. H.; Graham, S. Preparation and Characterisation of Some Nickel(II) Tetra-aza Macrocyclic Complexes Bearing Pendant Polymerisable Groups as Part of the Ligand Superstructure. *J. Chem. Soc., Dalton Trans.* **1989**, 1599−1608.

(32) Khokhar, A. R.; Deng, Y. J.; Kido, Y.; Siddik, Z. H. Preparation, Characterization, and Antitumor-Activity of New Ethylenediamine Platinum(IV) Complexes Containing Mixed Carboxylate Ligands. *J. Inorg. Biochem.* **1993**, *50*, 79−87; Chen, L.; Lee, P. F.; Ranford, J. D.; Vittal, J. J.; Wong, S. Y. Reduction of the Anti-Cancer Drug Analogue *cis*, *trans*, *cis*-[$PtCl_2(OCOCH_3)_2(NH_3)_2$] by L-cysteine and L-methionine and its Crystal Structure. *J. Chem. Soc., Dalton Trans.* **1999**, 1209−1212.

(33) Oxford Diffraction Ltd, Abingdon, OX144 RX, UK, CrysAlis RED. **2003**.

(34) Sheldrick, G. M. SHELXTL97, Structure Solution and Refinement Package, Universität Göttingen, Göttingen. **1997**.

(35) Altomare, A.; Burla, M. C.; Camalli, M.; Cascarano, G. L.; Giacovazzo, C.; Guagliardi, A.; Moliterni, A. G. G.; Polidori, G.; Spagna, R. SIR97: A New Tool for Crystal Structure Determination and Refinement. *J. Appl. Crystallogr.* **1999**, *32*, 115−119.

(36) Walker, N.; Stuart, D. An Empirical-Method for Correcting Diffractometer Data for Absorption Effects. *Acta Crystallogr., Sect. A. Found. Crystallogr.* **1983**, *39*, 158−166.

(37) Farrugia, L. J. Ortep-3 for Windows − A version of Ortep−III with a Graphical User Interface (GUI). *J. Appl. Crystallogr.* **1997**, *30*, 565.

JM0506468